IOP Conf. Series: Journal of Physics: Conf. Series **782** (2017) 012006 doi:10.1088/1742-6596/782/1/012006

Steady state operation simulation of the Francis-99 turbine by means of advanced turbulence models

A Gavrilov[1,2,3], A Dekterev[1,2,3] , A Minakov[1,2,3], D Platonov[1,2,3] and A Sentyabov[1,2,3]

[1] Siberian Federal University, Krasnoyarsk, Svobodniy 79, 660079 Russia
[2] Institute of Thermophysics SB RAS, Novosibirsk, Lavrentyeva 1, 630090 Russia
[3] Novosibirsk State University, Novosibirsk, Pirogova 2, 630090 Russia

E-mail: gavand@yandex.ru, dekterev@mail.ru, tov-andrey@yandex.ru, platonov-08@yandex.ru, sentyabov_a_v@mail.ru

Abstract. The paper presents numerical simulation of the flow in hydraulic turbine based on the experimental data of the II Francis-99 workshop. The calculation domain includes the wicket gate, runner and draft tube with rotating reference frame for the runner zone. Different turbulence models such as *k*-ω SST, *ζ-f* and RSM were considered. The calculations were performed by means of in-house CFD code SigmaFlow. The numerical simulation for part load, high load and best efficiency operation points were performed.

1. Introduction

Hydropower resources are the major renewable source of the electric power. At the present time, hydraulic power plants are being built and modernized. Accordingly, many scientific and engineering problems arise in the field of flow dynamics, such as finding of the power and efficiency of the turbine, calculation of the cavitation, pressure pulsations and forces on the turbine equipment.

Numerical simulation of flow in turbines is a useful tool for design of hydraulic turbines. At the same time, this is a very complicated problem due to complex shape of the flow path, turbulence, rotated runner, swirled flow under the runner and large-scale unsteady coherent structures. These features impose strict requirements on the turbulence models. Two-equation turbulence models (*k*-ε and *k*-ω) are most widely used in industrial applications. Large eddy simulation (LES) and hybrid RANS/LES methods are increasingly used for unsteady large-scale phenomena in complicated flows. At last, differential Reynolds stress model can accurately reproduce phenomena related to anisotropy of the turbulent fluctuations.

Several international projects were conducted for investigating flow in the hydraulic turbines with numerical simulation. The flow in the Kaplan turbine draft tube was considered in three Turbine-99 workshops. The Turbine-99 workshop organizing committee provide geometry of the draft tube, the experimental inlet velocity profiles and the other experimental data. Scientific groups performed a lot of steady and unsteady numerical simulations by means of different turbulence models: LES [1], DES [2], unsteady Spalart-Allmaras model [3] etc. However, the calculations strongly depends on the inlet conditions [4]. Another project of the turbine simulation was FLINDT. For example, in [5] numerical simulations of the rotating vortex were performed with the *k*-ε turbulence model in the compromise computational domain that includes runner and draft tube. A number of unsteady

approaches (URANS, DES, DDES and so on) were considered for numerical simulation of the flow in a test rig with stationary vertical guide vanes and a free runner [6].

Francis-99 is a project in the same spirit as the Turbine-99. It is a series of three workshops, which provides an open access of the complete design and data of a model Francis turbine [7]. Many scientist groups can use these data for validation of the different CFD codes and numerical approach. First workshop was in 2014 and 14 papers were presented. Those simulations were performed with *k*-ε, *k*-ω SST, SAS, RSM, zonal LES turbulence model and *k*-ω SST was the most widely used.

Previously, flow in the Francis-99 draft tube were simulated by means of the in-house CFD code SigmaFlow for the experimental data of the first workshop. Now, this paper presents an attempt of numerical simulation of the flow in the full turbine, including draft tube, runner and guide vanes, by means of the code SigmaFlow. The rotated reference frame approach validated for the code. Different turbulence models were considered for three operating points as well.

2. Mathematical model and numerical method

The simulations were based on the geometry and parameters of the operating points provided by organizers of the Francis-99 workshop II [7]. Computational domain consists of wicket gate, runner and draft tube (Fig. 1). Rotated reference frame in absolute velocity formulation was used for modeling of the runner rotation.

Below, the basic equations of the mathematical models expressing the conservation laws in the rotating reference frame are presented. Einstein summation convention is used.
The continuity equation (conservation of mass):

$$\frac{\partial u_i}{\partial x_i} = 0 \tag{1}$$

Momentum equations (conservation of momentum) in a rotating reference frame for absolute velocities:

$$\frac{\partial \rho u_i}{\partial t} + \frac{\partial}{\partial x_j}\left(\rho u_j^r u_i\right) = -\frac{\partial p}{\partial x_i} + \frac{\partial}{\partial x_j}(\tau_{ij}^{\mathrm{m}} + \tau_{ij}^{\mathrm{t}}) - \rho \varepsilon_{ijk}\Omega_j u_k \tag{2}$$

Where: u_i – absolute velocity components, u_j^r – relative velocity components, τ_{ij}^{m} – viscous stress tensor, τ_{ij}^{t} – turbulent stress tensor, Ω – angular velocity of runner rotation, p – static pressure, ρ – density, ε_{ijk} – Levi-Civita symbol. Several turbulence modeling approach were used. There were eddy viscosity models (*k*-ω SST, [8, 9], ζ-*f* [10]) and differential Reynolds stress model [11]. Pressure strain term is modeled by SSG strain model [11].

Due to the poor mesh, the computational domain did not include spiral case, therefore the head can not be used as a boundary condition. The discharge, obtained from the experimental data, was fixed at the inlet and outlet boundaries. The inlet velocity was directed normal to the wicket gate inlet. Speed of the runner rotation was -34.83 rad/s according to experimental parameters and the runner wall rotated with corresponding velocity. The density of the water was $\rho = 999.8$ kg/m^3 and the molecular viscosity was $\mu = 9.568 \cdot 10^{-4}$ Pa·s.

Computational meshes includes about 4.3 mln. polyhedral cells (see Table 1, Fig. 1, b). Dimensionless wall distance varied from 80 in the runner and draft tube cone up to 10^3 in the draft

tube tail. Standard wall function was used in case of eddy viscosity model and a blended technique [13] was used in case of RSM model.

Table 1. Mesh resolution

	Cells, mln. cells
Wicket gate	0.57
Runner	1.76
Draft tube	1.94

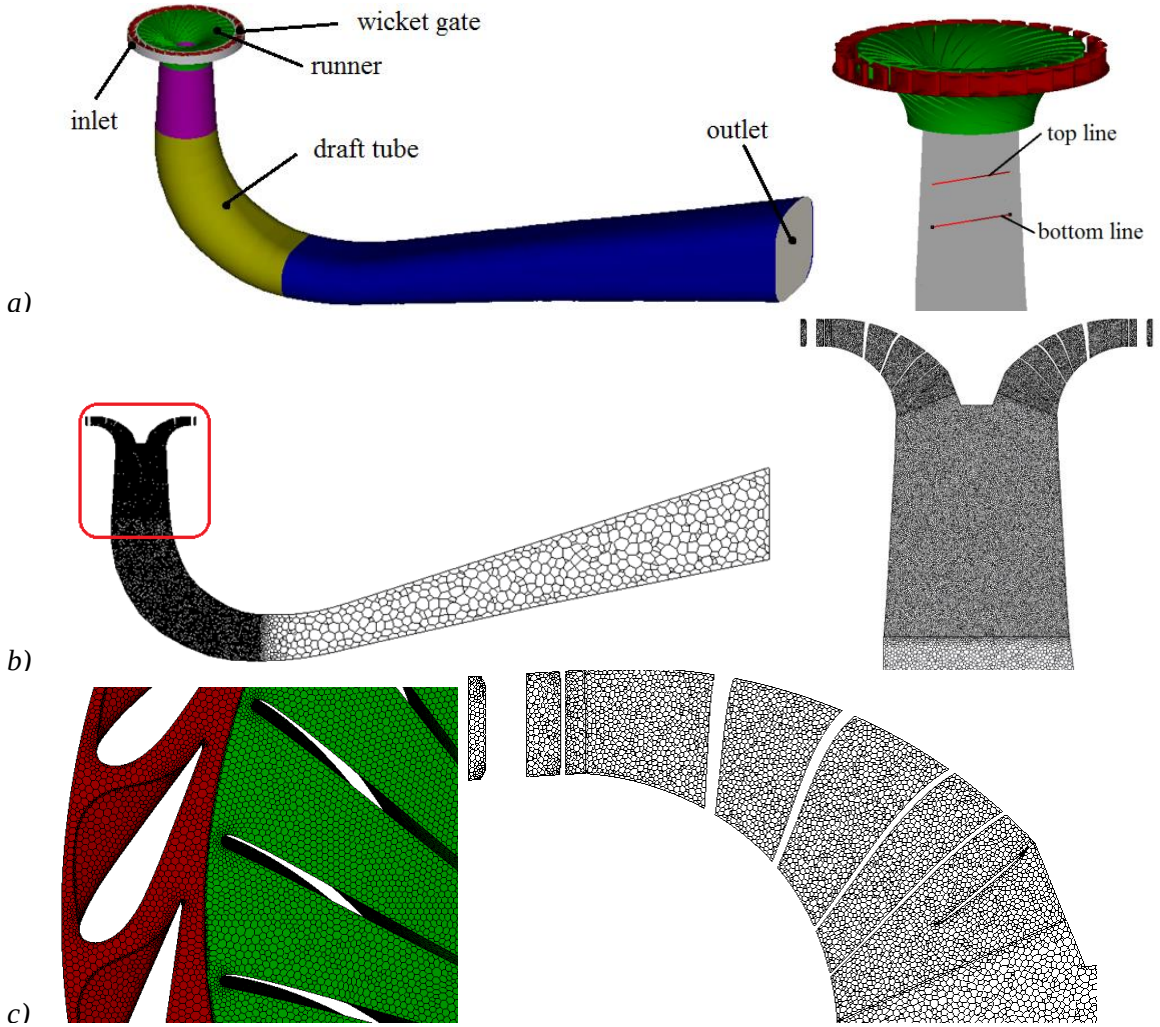

Figure 1. Francis-99 test case; *a*) computational domain; *b*) mesh in central cross-section, c) detailed views of the mesh on the guide vanes and the runner

The simulations were performed by means of in-house CFD code SigmaFlow [12, 13] which is developed in the Institute of thermophysics, Novosibirsk. The code was designed for solving of hydrodynamics and thermophysics problems in industrial applications and scientific investigations in the field of numerical simulation of turbulence, cavitation, non-Newtonian flow and heat transfer. Discretization of transport equations was carried out by the control volume method on unstructured

grids which can includes both hexahedral and polyhedral cells. Program package includes mesher and can use imported meshes. Analysis of the solution is performed by means of the built-in 3D visualizer. Parallel calculations are performed by means of domain decomposition and MPI.

Coupling of the velocity and pressure fields for incompressible flow was realized using the multistep SIMPLE-like procedure. Schemes of different order are available for the approximation of the convective terms in the equations for momentum components but in these calculation only up-wind scheme was used due to poor robustness. For the approximation of the convective terms in the equations for turbulent characteristics up-wind scheme was used as well. Unsteady calculation were performed to obtain steady or averaged solution. Time step was 0.01 s in case of *k*-ω SST and ζ-*f* turbulence models and 10^{-4} s in case of Reynolds stress model since RSM had worse convergence.

Earlier some calculations have shown that this technique can reliably consider averaged velocity and large-scale turbulent fluctuations in water turbines [8–9].

3. Results of Francis-99 simulations

In case of fixed discharge, the calculated torque on the runner is overestimated noticeably in the considered operating points (Table 2). Models *k*-ω SST and ζ-*f* calculates the same value of the torque, but RSM model obtains the lesser one. The discrepancies of the torque vary from 9 to 16%. Since the calculated torque is larger than experimental one the discrepancies is not seem a results of the mesh resolution. Fig. 2 shows that there is small difference of pressure distribution on the runner blades between *k*-ω SST and ζ-*f* results. Reynolds stress models demonstrates the same results near the leading edges of the blades but the flow around trailing edges is different (see Fig. 2, 3). In case of RSM, the region of the low pressure is localized on a small area near the leading edge (Fig. 3).

Table 2. Torque on the runner, N·m (discrepancies, %)

	PL	BEP	HL
k-ω SST	487 (16%)	703 (13%)	835 (12%)
ζ-*f*	486 (15%)	702 (13%)	833 (12%)
RSM	465 (10%)	680 (9%)	810 (9%)
experiment	421	621	744

At the best efficiency operating point, the flow under the runner is steady and weakly swirled (Fig 4*b*, 5*b*). There is small recirculation region under the runner hub. This zone generates long wake along the turbine axis. There is a straight weak vortex at the turbine axis. The axial velocity profiles have the maximum around the wake (Fig 4*b*, 6*b*). The calculated axial velocity profiles closely agree with the experimental profiles. There is no graphical differences between results of the eddy viscosity models (*k*-ω SST and ζ-*f*).

At the part load operating point, large-scale unsteady vortex rope forms under the runner (Fig 4*a*, 5*a*). There are many small vortices under the runner blades near the draft tube wall (Fig 5*a*). Calculated axial velocity profiles show a recirculation zone near the axis, but experimental profiles do not show it (Fig. 6*a*). Therefore, the calculated vertical velocity is significantly above the experimental one at the axis in case of all the models.

At the high load operating point, there is a weak vortex under the runner hub (Fig 4*c*, 5*c*). The vortex undergoes instability and has a spiral form at a distant of the runner. Calculated axial velocity profiles agree with experimental data but they show significant numerical viscosity for all the models (Fig. 6*c*).

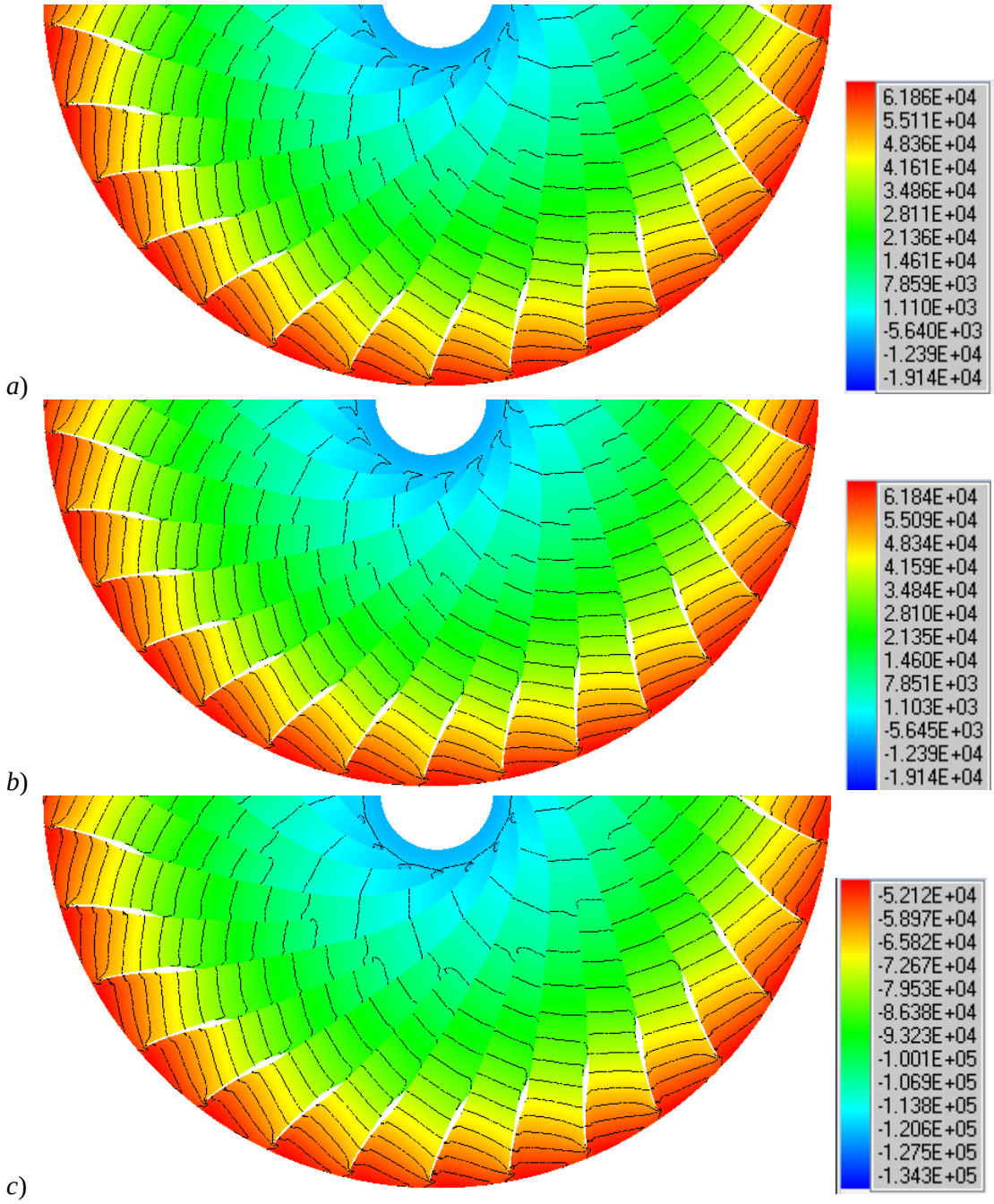

Figure 2. Pressure on the runner at the best efficiency point: *a*) *k*-ω SST; *b*) ζ-*f* , *c*) RSM

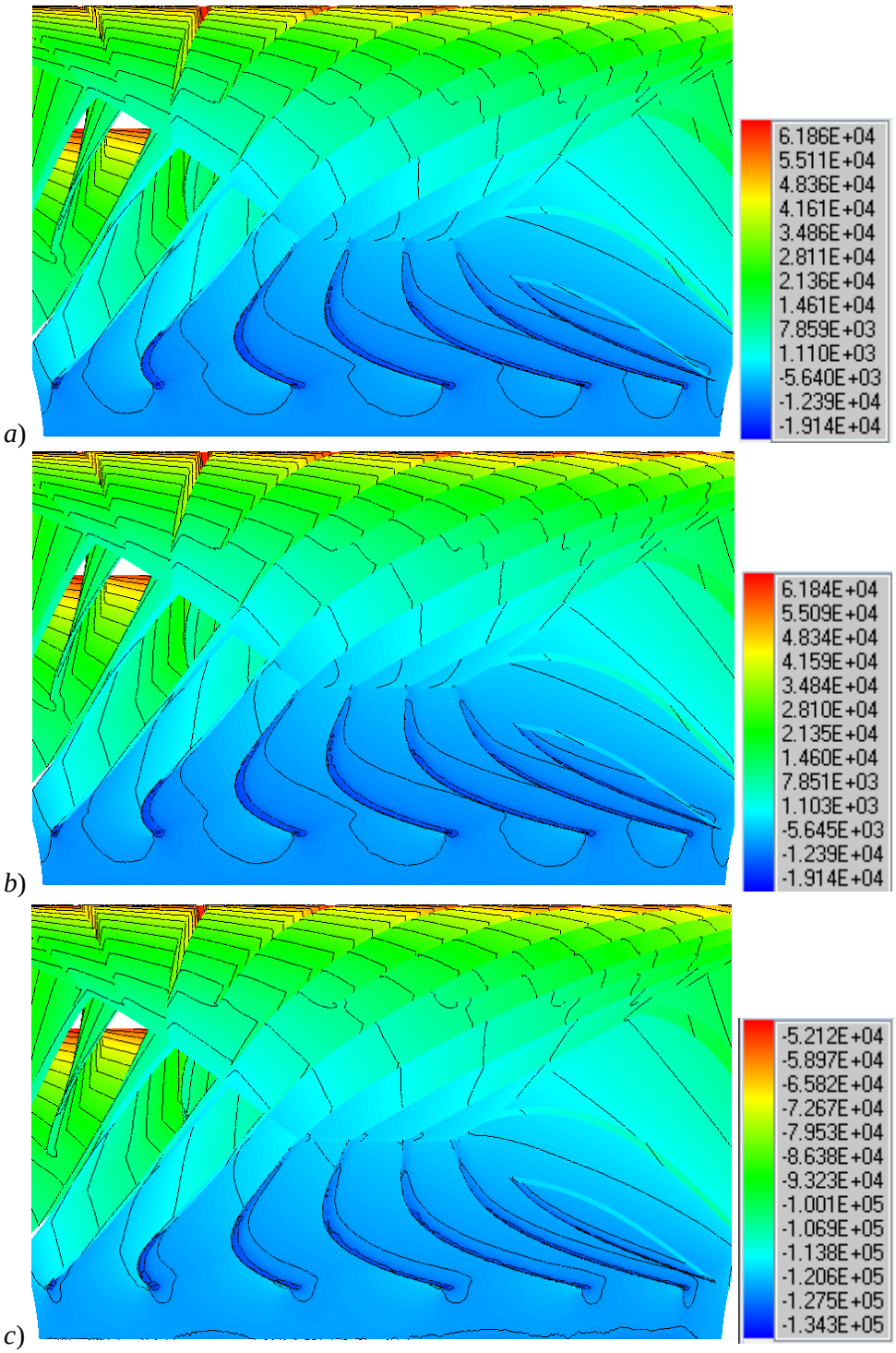

Figure 3. Pressure on the trailing edge of the runner blades at the best efficiency point: *a*) *k*-ω SST; *b*) ζ-*f* , *c*) RSM

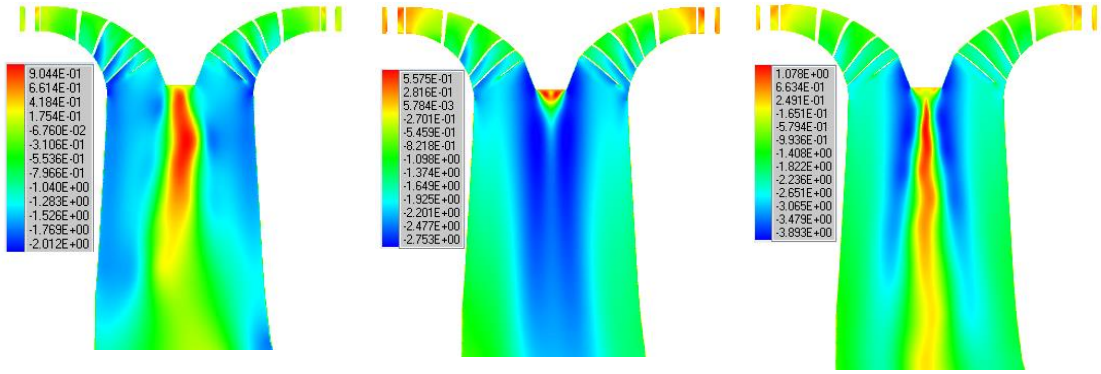

a *b* *c*

Figure 4. Instant vertical velocity in the central plane (ζ-*f* model): *a*) part load, *b*) best efficiency point, *c*) high load.

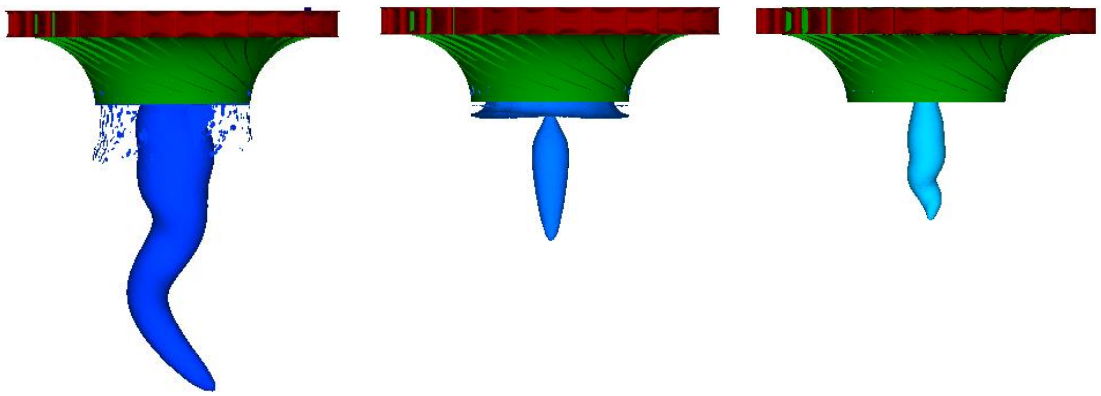

a *b* *c*

Figure 5. Vortices in the draft tube, visualized by iso-pressure surface (ζ-*f* model): *a*) part load, *b*) best efficiency point, *c*) high load.

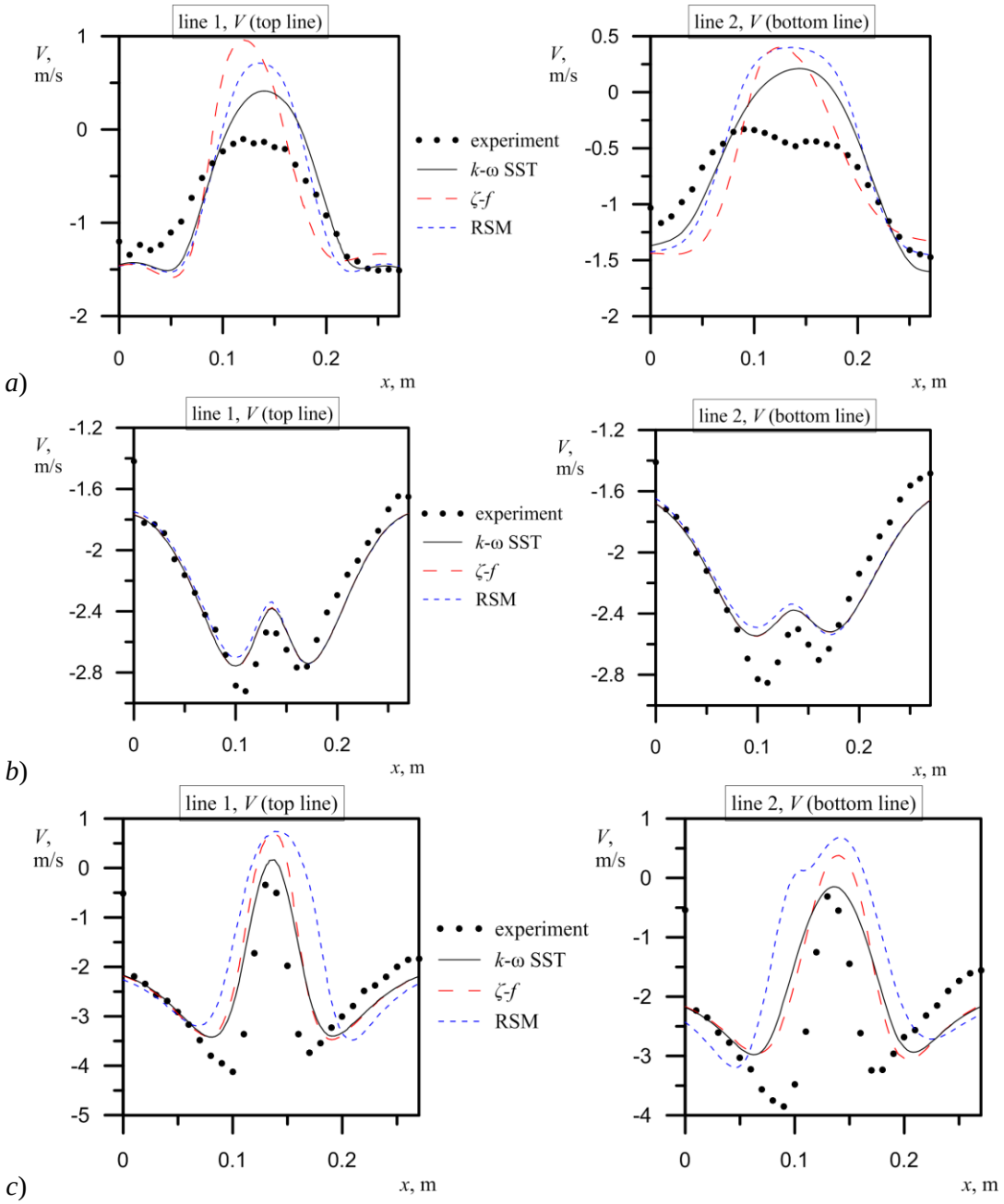

Figure 6. Averaged axial velocity component in the draft tube: *a*) part load; *b*) best efficiency point, *c*) high load.

4. Conclusions

Thus, this paper presents the first example of turbine simulation by means of the code SigmaFow in such formulation (wicket gate, rotor and draft tube with rotated reference frame for the runner zone). This kind of calculation is a challenge for the computational resources. For example, eddy viscosity simulations takes several days computation by means of 24 CPU cores.

The calculations show flow patterns depending on the operating point of the turbine. At the best efficiency point the flow in the draft tube is steady and there is a weak straight vortex along the turbine axis under the runner. At part load operating point there is a wide strong vortex rope that rotates near

the draft tube wall. At high load operating point there is a weak vortex under the runner hub which form becomes spiral at a distant of the runner.

Three modern turbulence models were considered. *k*-ω SST model is one of the most widely used in industrial applications and robust model. ζ-*f* model is an advanced four-equation model that can accurately describe near wall turbulence. Differential Reynolds stress model is a promising tool in case of complex, especially swirled, turbulence flow. There are still many unresolved problems off Reynolds stress model related to wall function, robustness, computational efficiency and so on.

The calculated data agree with experimental results well for best efficiency point. For high load operating points there is only qualitative agreement between calculation and experimental results. For part load operating points there is significant discrepancy between calculated and experimental results. For all the regimes there is no noticeable difference between the results of the eddy viscosity models *k*-ω SST and ζ-*f*.

Acknowledgements
This work was supported by Russian Science Foundation (project No. 16-19-00138).

References

[1] Kurosava S and Nakamura K 2005 Unsteady turbulent flow simulation in T99 draft tube *Proceedings of the third IAHR/ERCOFTAC workshop on draft tube flows Turbine 99* pp. 73–82.
[2] Marjavaara D.B., Kamakoti R., Lundstrom T.S.,Thakur S., Wright J. and Shyy W. 2005 Steady and unsteady CFD simulation of the Turbine-99 draft tube using CFX-5 and Stream *Proceedings of the third IAHR/ERCOFTAC workshop on draft tube flows Turbine 99* pp. 83–99.
[3] Page M., Giroux A.M. and Nicolle J. 2005 Steady and unsteady computation of Turbine-99 draft tube *Proceedings of the third IAHR/ERCOFTAC workshop on draft tube flows Turbine 99* pp. 109–124.
[4] Nilsson H. 2006 Evaluation of OpenFOAM for CFD of turbulent flow in water turbines *Proceedings of 23rd IAHR Symposium*
[5] Ciocan G.D. Iliescu M.S., Vu T.C., Nennemann B. and Avellan F. 2007 Experimental Study and Numerical Simulation of the FLINDT Draft Tube Rotating *Transactions of the ASME* **129** pp. 146 – 158
[6] Javadi A and Nilsson H 2015 Time-accurate numerical simulations of swirling flow with rotor-stator interaction *Flow, Turbulence and Combustion* **95(4)** pp 755 – 754 DOI: 10.1007/s10494-015-9632-2
[7] https://www.ntnu.edu/nvks/test-case.
[8] Menter F R 1994 Two equation eddy viscosity turbulence models for engineering applications *AIAA J.* **32(8)** pp 1598-1605
[9] Menter F R, Kuntz M and Langtry R 2003 Ten years of experience with the SST turbulence model *Heat and Mass Transfer* **4** pp 625–632
[10] Hanjalić K, Popovac M and Hadžiabdić M 2004 A obust near-wall elliptic relaxation eddy viscosity turbulence model for CFD *Int. J. Heat Fluid Flow* **25(6)** pp 1047-1051.
[11] Speziale C G, Sarkar S and Gatski TB 1991 Modeling the pressure–strain correlation of turbulence: an invariant dynamical system approach *J. Fluid Mech.* **227** pp 245-272.
[12] Gavrilov A A, Dekterev A A and Sentyabov A V 2015 Modeling of swirling flows with coherent structures using the unsteady reynolds stress transport model *Fluid Dynamics* Vol. **50(4)** pp 471 – 482.
[13] Gavrilov A A, Sentyabov A V, Dekterev A A and Hanjalic K 2016 Vortical structures and pressure pulsations in draft tube of a Francis-99 turbine at part load: RANS and hybrid

RANS/LES analysis *International Journal of Heat and Fluid Flow* **June** (online available), DOI: 10.1016/j.ijheatfluidflow.2016.05.007

[14] Minakov A V, Platonov D V, Dekterev A A, Sentyabov A V and Zakharov A V 2015 The numerical simulation of low frequency pressure pulsations in the high-head Francis turbine *Computers and Fluids* **111** pp 197-205, DOI:10.1016/j.compfluid.2015.01.007
Minakov A V, Platonov D V, Dekterev A A, Sentyabov A V and Zakharov A V 2015 The analysis of unsteady flow structure and low frequency pressure pulsations in the high-head Francis turbines *International Journal of Heat and Fluid Flow* **53** pp 183-194, DOI: 10.1016/j.ijheatfluidflow.2015.04.001